Journal of Alloys and Compounds 488 (2009) L30–L34

Contents lists available at ScienceDirect

Journal of Alloys and Compounds

journal homepage: www.elsevier.com/locate/jallcom

Letter

The isothermal oxidation behaviors of as-deposited and heat-treated Ni–11.5Cr–4.5Co–0.5Al sheet by EB-PVD at 800 °C

Li Mingwei[a,*], Zeng Gang[b], He Fei[c], He Xiaodong[c]

[a] National Key Lab for Precision Heat Processing of Metal, Harbin Institute of Technology, Harbin 150001, China
[b] School of Materials Science and Engineering, Harbin Institute of Technology, Harbin 150001, China
[c] Center for Composite Materials, Harbin Institute of Technology, Harbin 150001, China

ARTICLE INFO

Article history:
Received 12 November 2008
Received in revised form 27 August 2009
Accepted 30 August 2009
Available online 4 September 2009

Keywords:
Nickel-based superalloy
Electron beam physical vapor deposition
Oxidation

ABSTRACT

The isothermal oxidation behaviors for the as-deposited and heat-treated Ni–11.5Cr–4.5Co–0.5Al sheet by EB-PVD were investigated. The annealed of sheet was carried out at 800 °C for 16 h in 5×10^{-3} Pa. The oxidation exposures were conducted on electrical resistance furnace in 1 atm of laboratory air at 800 °C up to 120 h. The mass gain during subsequent oxidation was measured using a microbalance with a resolution of 10^{-5} g. Surfaces and cross-sections of the oxidized specimens were studied by scanning electron microscopy (SEM). Phase identification of the oxide scale was performed by glancing angle X-ray diffraction (GAXRD) and Energy Dispersive Analysis of X-rays (EDAX). The results show the heat-treated sheet with identical composition exhibited much more stable oxidation behavior than the as-deposited sheet. At 800 °C after 96 h isothermal exposure, the oxide scales of as-deposited sheet consisted mainly of an external NiO layer, a middle NiO and $NiCr_2O_4$ mixed layer and internal rich-Cr_2O_3 contained cobalt oxide layer. But those of heat-treated sheet exhibits NiO and Cr_2O_3 mixed layer with <1 μm thickness.

1. Introduction

The superior performance of superalloys was well known for their applications at high temperature and under severe environmental conditions. For an oxidation resistant superalloy, it is necessary and important to have good resistance to oxidation at high temperatures. The oxidation resistance of these alloys depends on the selective oxidation of reactive elements forming stable and slowly growing protective oxides such as Al_2O_3, Cr_2O_3 and SiO_2 [1].

The influence of alloy grain size on the oxidation behavior of these materials was important. It has been reported, this parameter affected importantly the oxidation resistance of several materials such as Ni-based superalloys or PM2000 alloys [2–6], especially for micro- or nano-crystalline alloy, at which grain boundaries could act as rapid diffusion pathways for the different reacting elements. Generally, oxide scales formed on high Cr alloys were multi-layered and the kinetics was strongly influenced by the alloy grain boundaries. Wang et al. [2], Yang and Wang [3] and Lou et al. [4] have performed extensive research on the oxidation behavior of sputtered Ni-base nanocoatings (grain size below 100 nm) with a composition identical to that of the underlying substrate alloys, indicating that the nanocoatings altered oxidation behavior and possessed much better oxidation resistance than the uncoated alloys.

The microcrystal superalloy sheets could be fabricated by electron beam physical vapor deposition (EB-PVD) method because the technique can provide deposition rate up to 100 nm/s. And the materials produced by EB-PVD technique are dense with controlled compositions and microstructures [7,8]. In the present study, a comparison of the isothermal oxidation behavior of as-deposited and heat-treated (at 800 °C for 16 h) microcrystalline Ni–11.5Cr–4.5Co–0.5Al superalloy sheet by electron beam physical vapor deposition (EB-PVD) at 800 °C in air was investigated.

2. Experimental

The materials used in this study are Ni–11.5Cr–4.5Co–0.5Al (wt%) superalloy sheets (0.3 mm in thickness) that have been produced by the electron beam physical vapor deposition technique (EB-PVD). And heat-treated samples annealed at 800 °C in 5×10^{-3} Pa for 16 h. And the average grain size of the as-deposited strip was about 500 nm. Therefore, it can be named as microcrystalline alloy. Fig. 1 shows the TEM Micrograph of as-deposited (Fig. 1a) and SEM Micrograph (Fig. 1b) heat-treated Ni–11.5Cr–4.5Co–0.5Al superalloy sheet by EB-PVD.

Rectangular coupons of 20 mm × 20 mm were cut by linear cutting machine. The surface was polished through 600 grit silicon carbide grinding paper. A hole of 1 mm in diameter was drilled on the samples for oxidation test. The specimens were hung within the reaction chamber of an electrical resistance furnace by a thin platinum wire. The oxidation exposures were conducted on electrical resistance furnace in 1 atm of laboratory air at 800 °C up to 120 h. The specimen was introduced directly into the hot-zone. After exposure, samples were left to cool down out of the furnace and, then, weighed. The weight gains per exposed area (g/mm^2) were measured on a microbalance with a resolution of 10^{-5} g.

* Corresponding author. Tel.: +86 451 86418834.
E-mail address: limingwei71@163.com (L. Mingwei).

0925-8388/$ – see front matter © 2009 Elsevier B.V. All rights reserved.
doi:10.1016/j.jallcom.2009.08.142

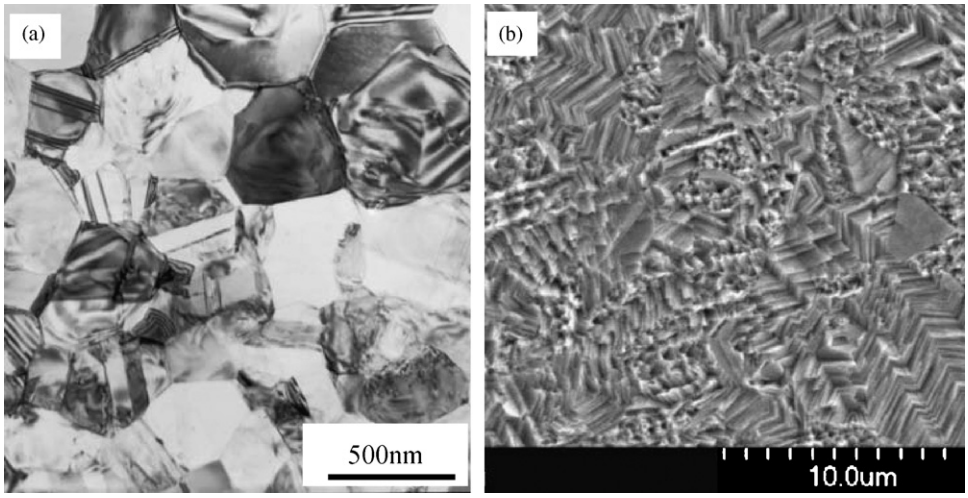

Fig. 1. TEM Micrograph of as-deposited (a) and SEM Micrograph heat-treated (b) Ni–11.5Cr–4.5Co–0.5Al superalloy sheet by EB-PVD.

After oxidation, the specimens were examined by both scanning electron microscopy (SEM) equipped with an energy dispersive X-ray microanalysis (EDX) system and cross-section metallography. Phase identification of the oxide scales was performed by glancing angle X-ray diffraction (GXRD). Cross-sections were prepared by conventional metallographic techniques, without alumina grinding media.

3. Results

3.1. Oxidation kinetics

Fig. 2 shows the results of isothermal oxidation tests for the as-deposited and heat-treated Ni–11.5Cr–4.5Co–0.5Al sheet by electron beam physical vapor deposition (EB-PVD). The isothermal oxidation tests were conducted at 800 °C in air. While the as-deposited Ni–11.5Cr–4.5Co–0.5Al sheet showed a rapid increase of mass gain, the heat-treated sheet with identical composition exhibited much more stable oxidation behavior than the as-deposited sheet.

3.2. Surface morphology

Fig. 3 shows SEM images of surface oxides of the as-deposited and after heat-treated Ni–11.5Cr–4.5Co–0.5Al sheet after isothermal oxidation at 800 °C for 2 h.

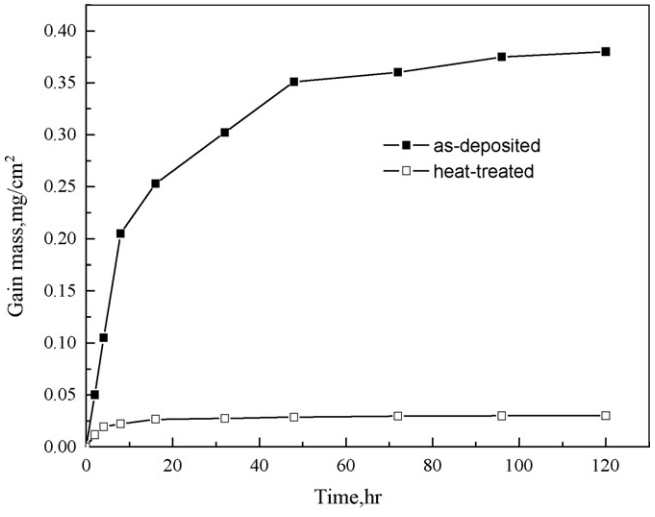

Fig. 2. The mass gain vs. time plots for the as-deposited and heat-treated microcrystalline Ni–11.5Cr–4.5Co–0.5Al superalloy sheet at 800 °C up to 120 h.

Fig. 4 shows SEM images of surface oxides of the as-deposited and after heat-treated Ni–11.5Cr–4.5Co–0.5Al sheet after isothermal oxidation at 800 °C for 48 h. Nonprotective Ni-oxides were dominantly observed in the as-deposited Ni–11.5Cr–4.5Co–0.5Al sheet, which exhibited poor oxidation behavior, whereas Cr_2O_3 oxide resulting in improved oxidation resistance was observed together with Ni-oxides in the heat-treaded Ni–11.5Cr–4.5Co–0.5Al sheet. In fact, the Cr_2O_3 and NiO mixed oxide was dominant layer through whole surface of the heat-treaded Ni–11.5Cr–4.5Co–0.5Al sheet, and, in Fig. 3b, the fraction of Ni-oxides was not so high. Therefore, the dominant Cr_2O_3 formation in the heat-treaded Ni–11.5Cr–4.5Co–0.5Al sheet gave rise to very low oxidation rate in Fig. 2. The phase identification in Fig. 7 for the surface oxides shows good agreement with the oxide morphologies displayed in Fig. 3. Cr_2O_3 oxide resulting in improved oxidation resistance was observed together with Ni-oxides in the heat-treaded Ni–11.5Cr–4.5Co–0.5Al sheet. In fact, the Cr_2O_3 and NiO mixed oxide was dominant layer through whole surface of the heat-treaded Ni–11.5Cr–4.5Co–0.5Al sheet, and, in Fig. 3b, the fraction of Ni-oxides was not so high. Therefore, the dominant Cr_2O_3 formation in the heat-treaded Ni–11.5Cr–4.5Co–0.5Al sheet gave rise to very low oxidation rate in Fig. 2. The phase identification in Fig. 7 for the surface oxides shows good agreement with the oxide morphologies displayed in Fig. 3.

3.3. Cross-sectional views

Figs. 5 and 6 shows representative images of the surface scales obtained by SEM. In general, the scales of as-deposited sheet were <3 μm thick and that of heat-treated sheet were <1 μm thick at 800 °C. And scales were adherent to the alloy. Both states resulted in scales having fairly rough surfaces.

From Fig. 5, the oxide scale formed on the as-deposited Ni–11.5Cr–4.5Co–0.5Al superalloy at 800 °C after 96 h isothermal exposure presented an irregular scale/alloy interface with relatively uniform thicknesses. After 96 h oxidation at 800 °C, the oxide of the as-deposited Ni–11.5Cr–4.5Co–0.5Al superalloy had a triple-layered microstructure. And exhibits an external NiO layer, a middle NiO and $NiCr_2O_4$ mixed layer and internal rich-Cr_2O_3 contained cobalt oxide layer.

From Fig. 6, the oxide scale formed on the heat-treated Ni–11.5Cr–4.5Co–0.5Al superalloy at 800 °C after 96 h isothermal exposure presented a smooth interface with relatively uniform thicknesses.

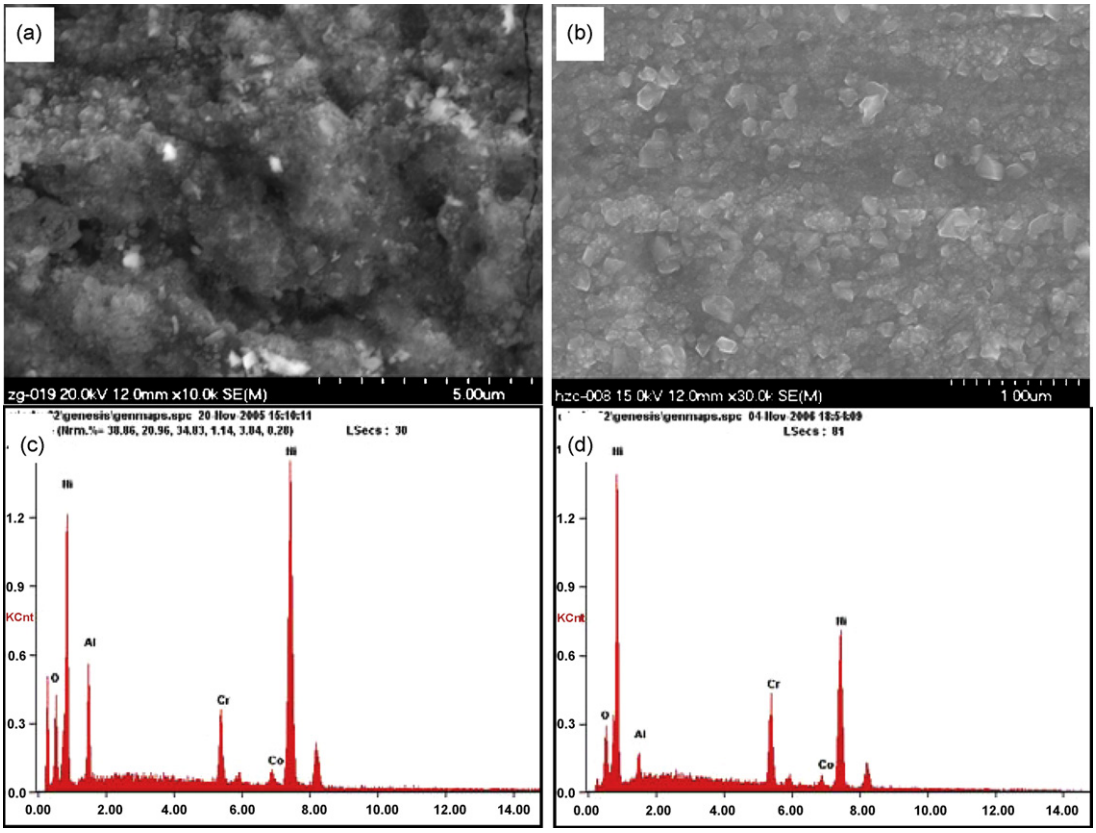

Fig. 3. SEM micrographs (a and b) and compositional analysis (c and d) of the surface morphology of as-deposited (a and c) and heat-treated (b and d) Ni–11.5Cr–4.5Co–0.5Al alloy after isothermal exposure in air at 900 °C for 2 h.

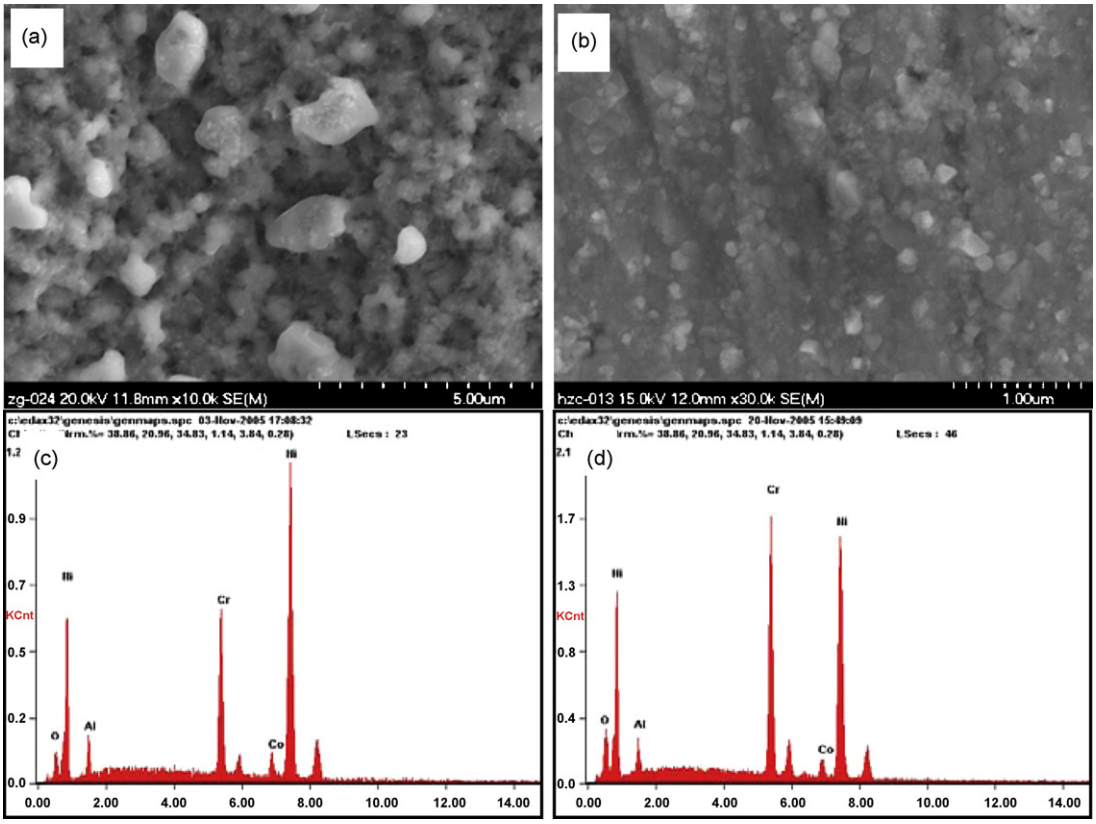

Fig. 4. SEM micrographs (a and b) and compositional analysis (c and d) of the surface morphology of as-deposited (a and c) and heat-treated (b and d) Ni–11.5Cr–4.5Co–0.5Al alloy after isothermal exposure in air at 900 °C for 48 h.

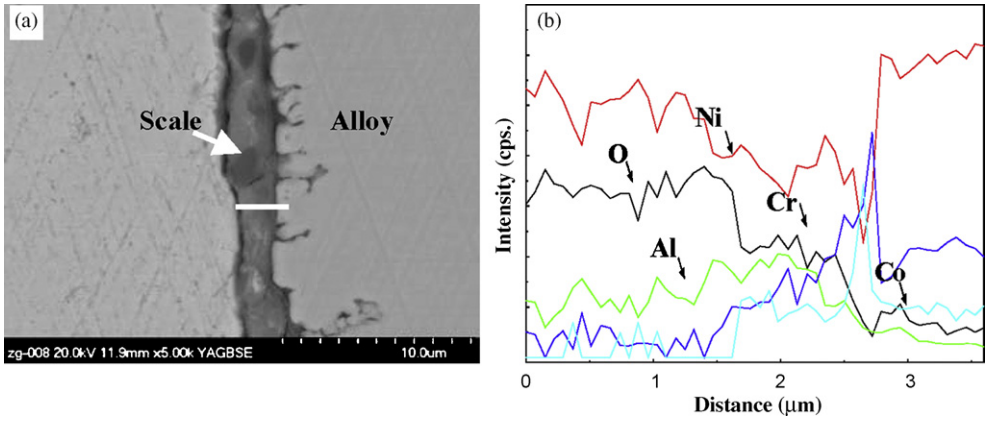

Fig. 5. (a) Cross-sectional of the scale and (b) line scanning of the as-deposited Ni–11.5Cr–4.5Co–0.5Al superalloy exposured at 800 °C for 96 h.

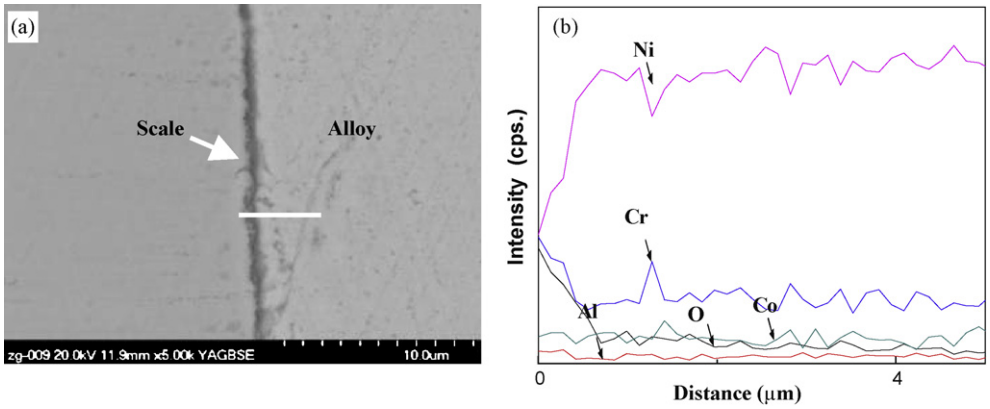

Fig. 6. (a) Cross-sectional SEM and (b) line scanning of heat-treated Ni–11.5Cr–4.5Co–0.5Al alloy at 800 °C for 96 h.

3.4. X-ray diffraction measurements

Fig. 7 shows the GAXRD diffraction spectra of the oxide scales on as-deposited and heat-treated superalloy at 900 °C after 96 h isothermal exposure.

The peaks of as-deposited superalloy were found from NiO, the underlying Ni matrix, $NiCr_2O_4$ with a minor amount of Cr_2O_3. But the peaks of heat-treated superalloy with a high intensity of the matrix were found, together with small peaks from Cr_2O_3, NiO and CrO_2.

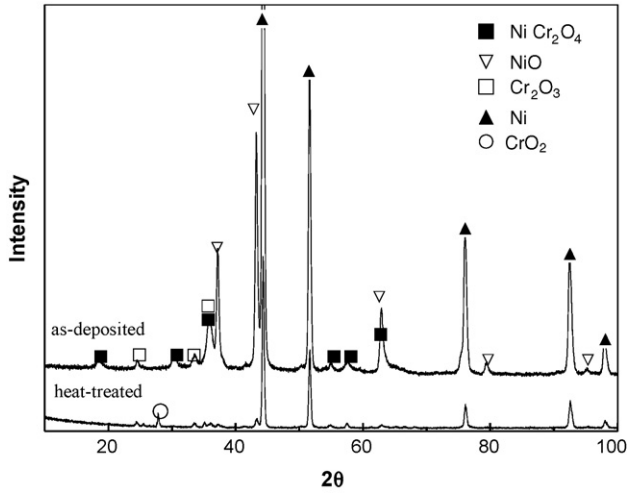

Fig. 7. XRD analysis of as-deposited and heat-treated Ni–11.5Cr–4.5Co–0.5Al superalloy sheet by EB-PVD exposured at 800 °C for 96 h in air.

4. Discussion

Chromia and alumina scales, which grow by grain-boundary diffusion, are the most important protective scales for high-temperature alloys [9]. In Ni-rich Ni–11.5Cr–4.5Co–0.5Al alloys, the selective oxidation of Cr should be promoted for Cr_2O_3 formation instead of Ni-oxides during exposure at high temperature. Kofstad, in his review [10] of the extensive data available for chromium oxidation, demonstrated that the Cr_2O_3 scale grows by counter-current diffusion of metal and oxygen along grain boundaries. And grain-boundary diffusion is much faster than lattice diffusion for both chromium and oxygen. Grain-boundary diffusion is often more important than lattice diffusion at low temperatures. A principal reason for this is the lower activation energy of the boundary process, corresponding to the more disordered structures in the boundaries. A second reason is the usually finer grain size and hence more numerous boundaries encountered at lower temperatures [11].

Moreover, rapid diffusion paths such as grain boundaries can significantly enhance the selective oxidation of Cr, which is necessary to form a protective scale on the entire surface, in order to prevent oxidation of the base material, e.g. Ni. Therefore, small grain size plays an important role in the formation of Cr_2O_3 oxides. The oxide grains were much smaller on both as-deposited and heat-treated microcrystalline Ni–11.5Cr–4.5Co–0.5Al superalloy

thereby higher density of grain-boundary acted as the routes of the short circuit diffusion could be existed in the oxide scale than that on coarse crystalline alloy.

But, the as-deposited Ni–11.5Cr–4.5Co–0.5Al superalloy sheet was produced by EB-PVD, the structure is nonequilibrium with excess vacancies which were frozen in during low energy deposition [12]. Nickel diffusion along grain boundaries and dislocations, which had approximately the same oxygen pressure dependence as that for lattice diffusion, takes place by the vacancy mechanism [13]. So, Ni can diffuse rapidly to surfaces, too. It can be confirmed from Fig. 4 that shows the results of elements distribution in scale. Obviously, it is disadvantageous for the formation of a protective Cr_2O_3 scale. In other words, the high diffusivity of the base materials elements of as-deposited sheet along substrate grain boundaries and other defects causes the more instable oxidation behavior than that of heat-treated sheet, which may significantly contribute to the elements transport toward the substrate/oxide interface in materials with small grain size and other defects such as voids. Namely, those elements diffuse too rapidly in as-deposited sheet substrate, which significantly reduced the selective oxidation of Cr. The more stable oxidation behavior of heat-treated Ni–11.5Cr–4.5Co–0.5Al sheet relative to that of as-deposited sheet can be explained by equilibrium microcrystalline structure effect.

Rapid diffusion paths such as grain boundaries can significantly help the selective oxidation of Cr, Al and consequent Cr_2O_3, Al_2O_3 formation, but the precise information about the elements flux resulting from the substrate grain boundaries and other defects would be necessary in order to enhance the selective oxidation.

5. Conclusions

The heat-treated sheet with identical composition exhibited much more stable oxidation behavior than the as-deposited sheet. The oxide scales of as-deposited sheet consisted mainly of an external NiO layer, a middle NiO and $NiCr_2O_4$ mixed layer and internal rich-Cr_2O_3 contained cobalt oxide layer. The scale of heat-treated sheet exhibits an external NiO and Cr_2O_3 mixed layer, a middle NiO layer and internal NiO and Cr_2O_3 mixed layer.

A slowly growing Cr_2O_3 oxide was observed on specimens with small grain size and equilibrium microcrystalline structure due to the high density of grain boundaries leading to fast outward Cr transport along the substrate grain boundaries.

Specimens with nonequilibrium microcrystalline structure form NiO growing outward and a mixed Cr, Co and Al oxide growing inward due to the high diffusivity of substrate elements, which significantly reduced the selective oxidation of Cr.

References

[1] X.J. Zhang, S.Y. Wang, F. Gesmundo, Y. Niu, Oxid. Met. 65 (2006) 152–165.
[2] F. Wang, X. Tian, Q. Li, L. Li, X. Peng, Thin Solid Films 516 (2008) 5740–5747.
[3] S.L. Yang, F.H. Wang, Oxid. Met. 65 (2007) 195–205.
[4] H.Y. Lou, F.H. Wang, S.L. Zhu, B.J. Xia, L.X. Zhang, Surf. Coat. Technol. 63 (1994) 105–114.
[5] P. Perez, Corros. Sci. 44 (2002) 1793–1808.
[6] M.C. Garcia-Alonso, J.L. Gonzalez-Carrasco, M.L. Escudero, J. Chao, Oxid. Met. 53 (2000) 77–98.
[7] A. Ustinov, L. Olikhovska, T. Melnichenko, A. Shyshkin, Surf. Coat. Technol. 202 (2008) 3832–3838.
[8] X.D. He, et al., J. Alloys Compd. 467 (2009) 347–350.
[9] P. Kofstad, Oxid. Met. 24 (1985) 265–276.
[10] P. Kofstad, High Temperature Corrosion, Elsevier Applied Science, London, 1988.
[11] D.J. Young, High Temperature Oxidation and Corrosion of Metals, Elsevier, London, 2008.
[12] K.S. Sree Harsha, Principles of Physical Vapor Deposition of Thin Films, Elsevier, London, 2008.
[13] P. Kofstad, Oxid. Met. 44 (1995) 3–27.